Electronic Supplementary Material (ESI) for Journal of Materials Chemistry A.

Supplementary Information

Operando evidence of Cu^+ stabilization via single-atom modifier for CO_2 electroreduction

Wei Zhang,[a] Peng He,[a] Chao Wang,[a] Tao Ding,[a] Tao Chen,[a,c] Xiaokang Liu,[a] Linlin Cao,[a] Tianming Huang,[a] Xinyi Shen,[a] Oleg A. Usoltsev,[d] Aram L. Bugaev,[d] Yue Lin*[b] and Tao Yao*[a]

[a] *National Synchrotron Radiation Laboratory, University of Science and Technology of China, Hefei 230029, P.R. China.*

[b] *Hefei National Laboratory for Physical Sciences at the Microscale, University of Science and Technology of China, Hefei, Anhui 230026, PR China.*

[c] *School of National Defense Science and Technology, Southwest University of Science and Technology, Mianyang, 621010, China*

[d] *The Smart Materials Research Institute, Southern Federal University, 178/24 Sladkova, 344090 Rostov-on-Don, Russia*

**Corresponding author.*
E-mail address: yaot@ustc.edu.cn; linyue@ustc.edu.cn

Experimental

Preparation of CuO nanosheets: A typical solvothermal method was used for the synthesis of CuO nanosheets. Generally, 40 g of NaOH and 7.33 g of hexadecyl trimethyl ammonium bromide (CTAB) were dissolved in 300 mL of deionized water, and then the mixture was transferred into a water bath and heated to 60 °C with vigorously magnetically stirring. Then 33 mL of $Cu(NO_3)_2{\cdot}3H_2O$ (1.33 g) solution was added dropwise into the mixture and continuous reaction for 1 h. The black products were collected by centrifugation and washed several times with deionized water and ethanol, and then dried under vacuum at 40 °C.

Preparation of Sn/CuO nanosheets: 100 mg as prepared CuO nanosheets were weighed and dispersed in a screw bottle with 50 mL water and ethanol (3:1) under continuous sonication for 30 mins to get a uniform dispersed solution. Then, 10 mL of $SnCl_4{\cdot}5H_2O$ aqueous solution (0.3 mg mL^{-1}) was dropped into the homogeneous CuO aqueous through microinjection pump and keeping stirring for 8 h at room temperature. The mixture was further collected by centrifugation and dried under vacuum at 40 °C.

Hydrogen reduction treatment: The obtained CuO and Sn/CuO nanosheets were transferred into the tube furnace and heated at 200 °C for 4h in hydrogen atmosphere, donated as CuO-H_2 and Sn/CuO-H_2, respectively.

Preparation of Cu_2O and Sn/Cu_2O nanosheets: The re-oxidation process was employed a solution treatment method. 10 mg as-prepared CuO-H_2 and Sn/CuO-H_2 nanosheets were weighed and dispersed in sample bottle with 2 mL water and ethanol (4:1) under continuous sonication for 1 h to form Cu_2O and Sn/Cu_2O nanosheets by the slow oxidation.

Characterization

Transmission electron microscopy (TEM) and energy dispersive X-ray spectra (EDS) analysis were performed on a JEOL-2100F transmission electron microscope at an accelerating voltage of 200 kV. The field emission scanning electron microscopy (SEM) images were taken on a Gemini SEM 500 scanning electron microscope. X-ray photoelectron spectroscopy (XPS) measurements was carried out on an ESCALAB

MKII instrument equipped with a Mg Kα source (hυ = 1253.6 eV). The binding energy scale of all measurements was calibrated by referencing C 1s to 284.5 eV. Powder X-ray diffraction (XRD) patterns were collected on Philips X'pert Pro Super diffractometer with Cu Kα line (λ = 1.5418 Å).

Soft X-ray XANES measurements

The Cu L_3-edge XANES measurements were performed at the BL10B beamline of NSRL. The bending magnet is connected to the beamline, which is equipped with three gratings covering photon energies from 100 to 1000 eV with an energy resolution of ca. 0.2 eV. The data were further recorded in the total electron yield mode by collecting the sample drain current. The resolving power of the grating was typically $E/\Delta E = 1000$, and the photon flux was 1×10^{-10} photons per second.

Operando XAFS measurements.

The Cu *K*-edge (8979 eV) and Sn *K*-edge (29200 eV) XAFS spectra were measured at the 14W1B beamline and 44A station of Shanghai Synchrotron Radiation Facility (SSRF) and Taiwan Photo Source (TPS). The storage ring of SSRF and TPS were operated at 3.5 and 3.0 GeV with a maximum electron current of 260 and 500 mA, respectively. The data were collected in transmission and fluorescence mode for Cu K-edge and Sn *K*-edge respectively. Operando XAFS measurements were conducted with the catalyst-modified carbon fiber paper (~1 cm×1 cm) as the working electrode and performed in a home-built cell for operando Quick-XAFS. Particularly, the catalyst powders were dispersed in 500 μL of ethanol, 500 μL of deionized water and 20 μL of Nafion solution (5 wt%, Sigma-Aldrich), and then ultrasonicated for 30 min. Subsequently, the well-distributed catalyst ink were drop-casted onto carbon fiber paper taped with polyimide film on the back, to ensure all of the electrocatalyst reacted with $KHCO_3$ electrolyte at a geometric metal loading of ~0.5 mg/cm^2. The operando XAFS spectra were collected through the transmission and fluorescence mode for Cu *K*-edge and Sn *K*-edge respectively.

First, the working electrode was tested through transmission mode without $KHCO_3$

electrolyte and applied voltage, and then named as Ex Situ. To further estimate the influence of $KHCO_3$ electrolyte, the working electrode was immersed in 0.1 M $KHCO_3$ at open circuit condition and the XAFS spectra were recorded also by transmission mode. To monitor the changes during CO_2RR process, the cathodic voltage was applied at -0.1 V, -0.6 V, -1.2 V and -1.8 V vs. RHE with the continuous spectrum collection of two spectra per minute. During the XAFS measurements, we seriously calibrate the position of absorption edge (E_0) using Cu foil and Sn foil, meanwhile, all the XAFS data were collected during one period of beam time. Moreover, each spectrum was measured three times to assure the repeatability of the data and the positions of E_0 are almost the same during the multiple scan. The position of E_0 is defined as the point corresponding to the maximum value in the derivative curves of the XANES spectra.

XAFS data analysis

Acquired EXAFS data were processed according to standard procedures using the ATHENA module implemented in the IFEFFIT software packages. The Cu *K*-edge k^3-weighted $\chi(k)$ and Sn *K*-edge k^2-weighted $\chi(k)$ data in the k-space ranging from 2.42 to 12.9 Å^{-1} and 2.55 to 11.2 Å^{-1} were Fourier-transformed to real (R) space using a Hanning windows (dk = 1.0 Å^{-1}) to separate the EXAFS contributions from different coordination shells, respectively. To obtain the detailed structural parameters around the Sn atom in the surfaces of Cu_2O nanosheets, quantitative curve fittings were carried out for the Fourier-transformed $k^2\chi(k)$ in R-space using the ARTEMIS module of IFEFFIT. Effective backscattering amplitudes F(k) and phase shifts $\Phi(k)$ of all fitting paths were calculated with the ab initio code FEFF8.054. For the Sn/Cu_2O sample, a k-range of 2.55–11.2 Å^{-1} was used and curve fittings were carried out in R-space within an R range of [1.0, 1.96] Å for k^2-weighted $\chi(k)$ functions. The number of independent points are:

$$Nipt = 2\Delta k \times \Delta R/\pi = 2 \times (11.2 - 2.55) \times (1.96 - 1.0)/\pi = 5$$

Compared with the Sn/Cu_2O-OCV sample, the FT curve showed an increase of peak intensity at 1.49 Å assigned to the Sn-O coordination, which was ascribed to be caused by the oxygen adsorption in the $KHCO_3$ electrolyte. Therefore, we conducted the single-shell structure model of a Sn-O shell to fit the EXAFS data of the sample at open circuit condition, where the Sn-O denotes the Sn atoms was anchored on the surface of Cu_2O nanosheets by coordinating with O atoms. During curve fittings, each of the Debye-Waller factors (σ^2) coordination numbers (CN), interatomic distances (R) and energy shift (ΔE_0) were treated as adjustable parameters for the Sn-O path.

Statistical analysis

Determination of the number of different copper species formed under reaction conditions and their concentration profiles were obtained using principle component analysis (PCA) module of PyFitIt program.[1] The procedure consists of two steps. At the first step, the eigenvalues of the covariance matrix associated to the input dataset are obtained and then used to calculate different statistical estimators, including factor indicator (IND) and imbedded error (IE) functions,[2] and Malinowski F-test.[3] Then, the target transformation procedure is applied to abstract PCA components to retrieve the chemically relevant spectra and their concentration profiles.

Calculation Details

The adsorption energy for CO on Cu (111) surface of Sn/Cu_2O NS and pure Cu (111) surface was calculated with the density functional theory (DFT) implemented in the Quantum Espresso software package.[4] Projected augmented wave (PAW) method and generalized gradient approximation (GGA) in the Perdew-Burke-Ernzerhof (PBE) parametrization were used to describe the electron-ion interaction and electron exchange-correlation. The DFT-D3 scheme was employed to describe the long-range van der Waals interactions. The kinetic energy cutoffs were 75 and 500 Ry for the plane wave and electron density. A $6\times6\times1$ k-grid was used for the Brillouin zone integration. The adsorption of CO on Cu (111) surface of Sn/Cu_2O NS and pure Cu (111) surface were both modeled based on a 4-layered Cu (111) slab model containing 64 Cu atoms with a vacuum layer of 18 Å along the z direction. The bottom 2 layers of the slab model were fixed to simulate the bulk Cu; and the top 2 layers and adsorbate were relaxed until all the atomic forces were less than 0.04 eV/Å.

Operando SR-FTIR spectroscopy measurements

Operando SR-FTIR spectroscopy measurements were conducted at the beamline BL01B of National Synchrotron Radiation Laboratory (NSRL) via a homemade top-plate cell reflection infrared set-up with a ZnSe crystal as the infrared transmission window with cutoff wavenumber of ~ 625 cm^{-1} (Fig. S14). This end station was equipped with an FT-IR spectrometer (Bruker 66 v/s) with a KBr beam-splitter and various detectors (here a liquid nitrogen cooled mercury cadmium telluride detector was used) coupled with an infrared microscope (Bruker Hyperion 3000) with a ×16 objective, and can provide infrared spectroscopy measurement with a broad range from 15 to 4000 cm^{-1} with a high spectral resolution of 0.25 cm^{-1}.

Electrochemical measurement

All electrochemical measurements were carried out in a three-electrode system. The gas-tight H-cell system was fabricated with a CO_2 gas compartment and two liquid compartments with channels of dimensions (Fig. S20). The catholyte and anolyte were separated by a proton exchange membrane. All potentials were measured against an Ag/AgCl reference electrode and converted to the reversible hydrogen electrode (RHE) scale by:

$$E \text{ (vs. RHE)} = E \text{ (vs. Ag/AgCl)} + 0.197 \text{ V} + 0.0592 \times \text{pH}.$$

The measured currents were normalized to the geometric surface area of the used carbon fiber paper. A steady supply of CO_2 gas was delivered at a rate of 20.0 sccm. Then effluent gas is collected by an air bag and injected into gas chromatography. During chronoamperometry, effluent gas went through the sampling loop of a gas chromatograph (SRI) and was analysed in 30 min intervals to determine the concentration of gas products. Gas products were analyzed by a thermal conductivity detector (TCD) (for H_2) and a flame ionization detector (FID) (for CO, alkanes and alkenes). Quantification of the products was performed using standard calibration gases. Liquid products were analyzed by quantitative ^{1}H NMR spectroscopy with water suppression, and using dimethyl sulphoxide (DMSO) as an internal standard. The Faradaic efficiency (FE) of gas and liquid products were calculated as:

$i_{co}=V_{co}*Q*2*F*P_0/(RT)$; $FE_{co}= i_{co}/i_{total}*100\%$; mass activity=$FE_{co}*i_{total}/(\beta*m_{cat})$ respectively, where i_{total} is measured current, F is Faradaic constant, p_0 is pressure, T is temperature and R is ideal gas constant, 8.314 J mol K^{-1}, β is Cu_2O or Sn/Cu_2O weight ratio in total carbon-supported NP catalysts, m_{cat} is catalyst weight. FEs were calculated from the amount of charge passed to produce each product divided by the total charge passed at a specific time or during the overall run (for liquid products). Relative turnover was compared based on the partial current density for each product. Mass activities were calculated based on the overall mass of Cu and Sn for each nanosheets and the mass loading was determined assuming complete hexagonal packing on the substrate. Each measurement was conducted three times to check the consistency of our experiments. Electrochemical data presented here are the average values out of these multiple measurements.

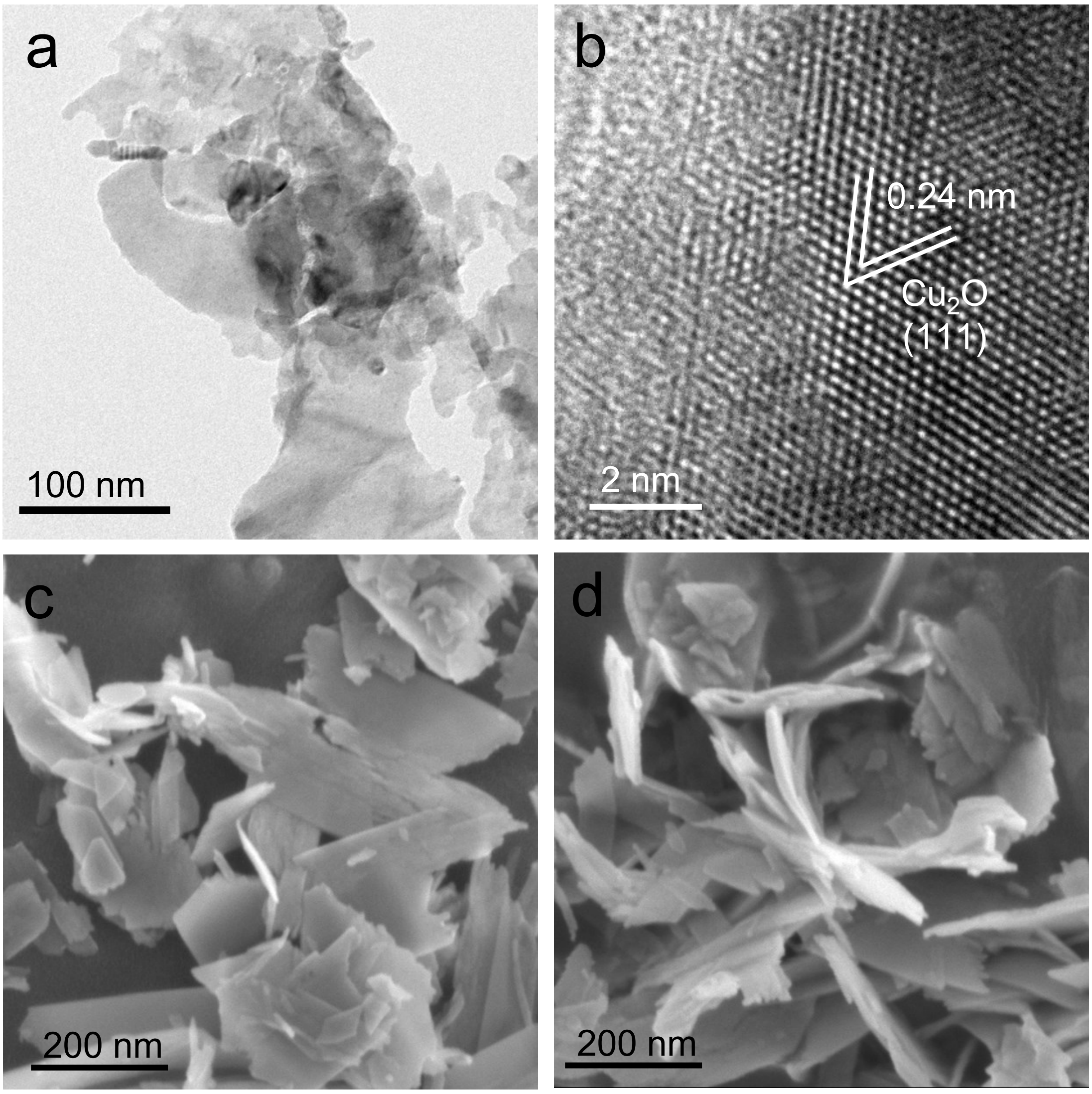

Figure S1. (a and b) High-resolution TEM images of the pure Cu_2O nanosheets. (c and d) Scanning electron microscope (SEM) images of Cu_2O and Sn/Cu_2O nanosheets, respectively.

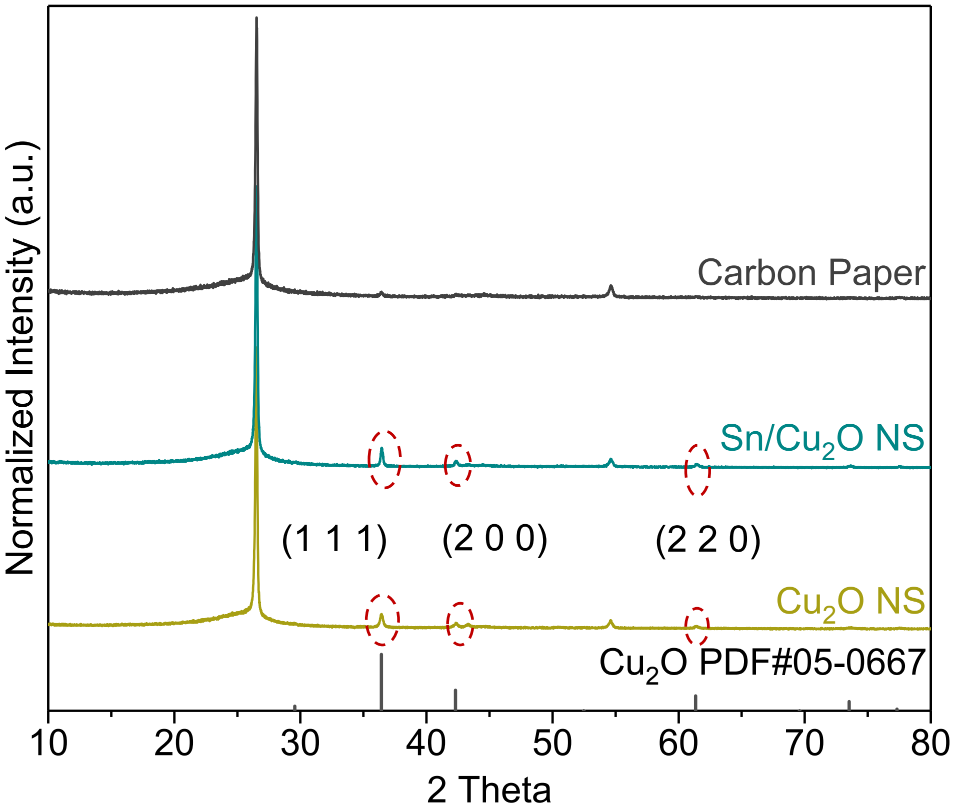

Figure S2. The XRD patterns of pure carbon paper and Cu_2O, Sn/Cu_2O loaded on carbon paper before CO_2RR.

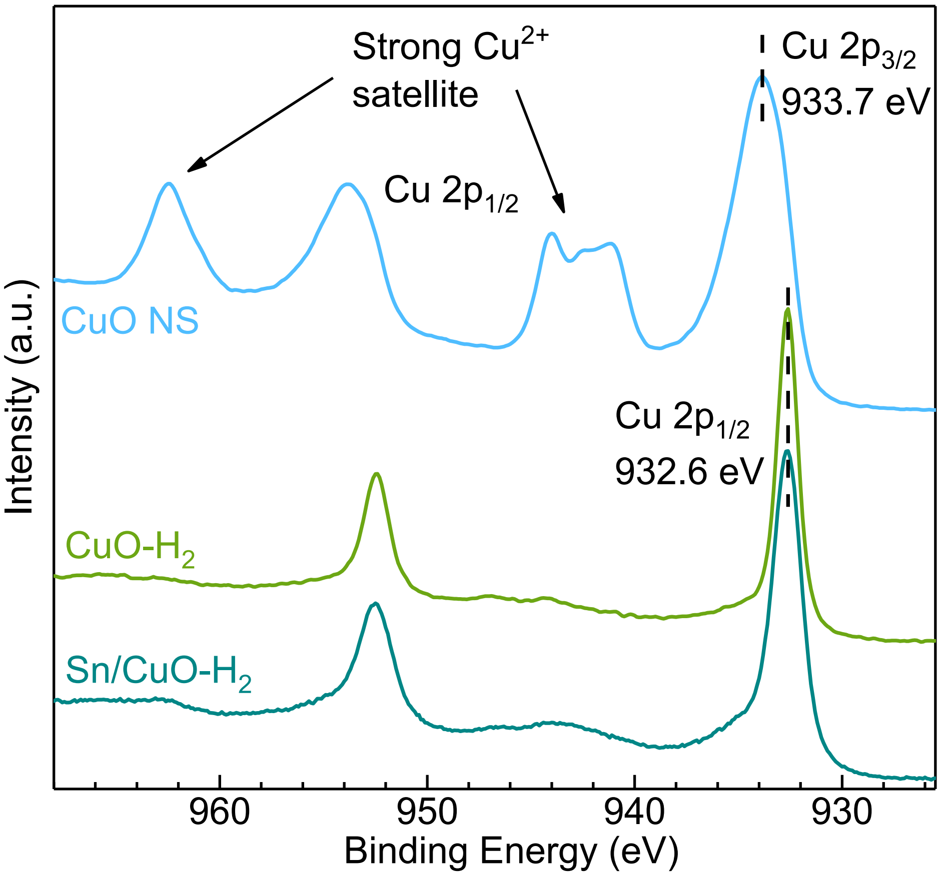

Figure S3. XPS regional spectra for Cu 2p of CuO, CuO-H_2 and Sn/CuO-H_2.

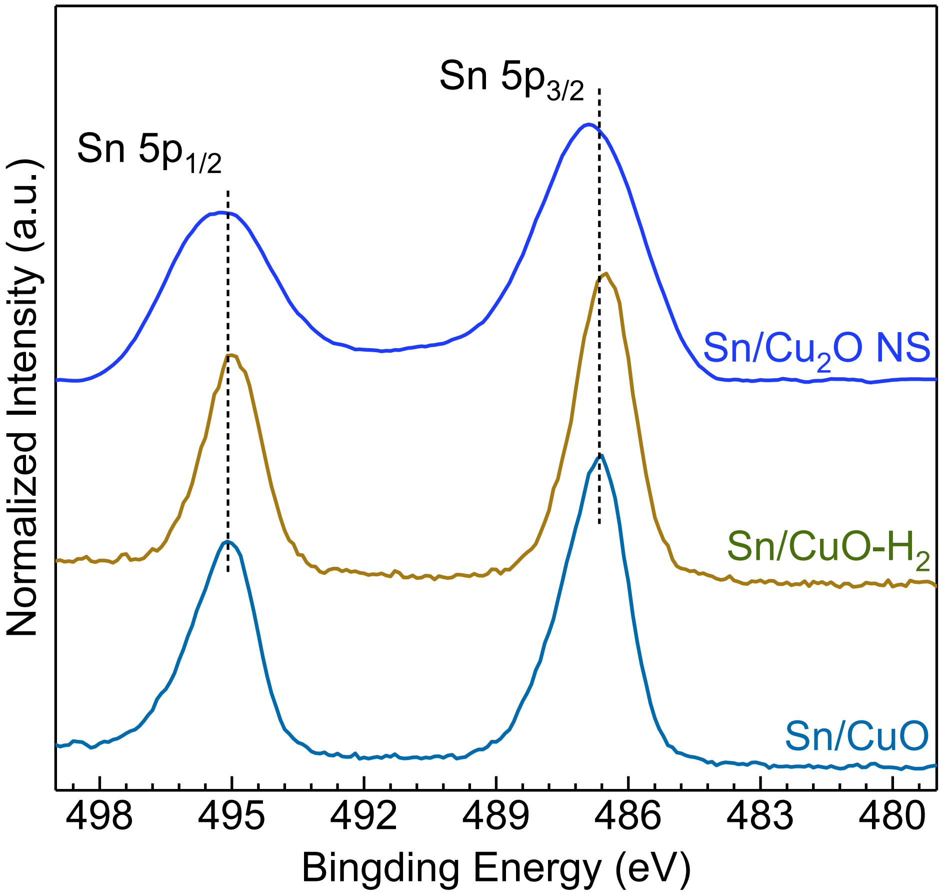

Figure S4. XPS regional spectra for Sn 5p orbit of Sn/CuO, Sn/CuO-H_2 and Sn/Cu_2O after reaction.

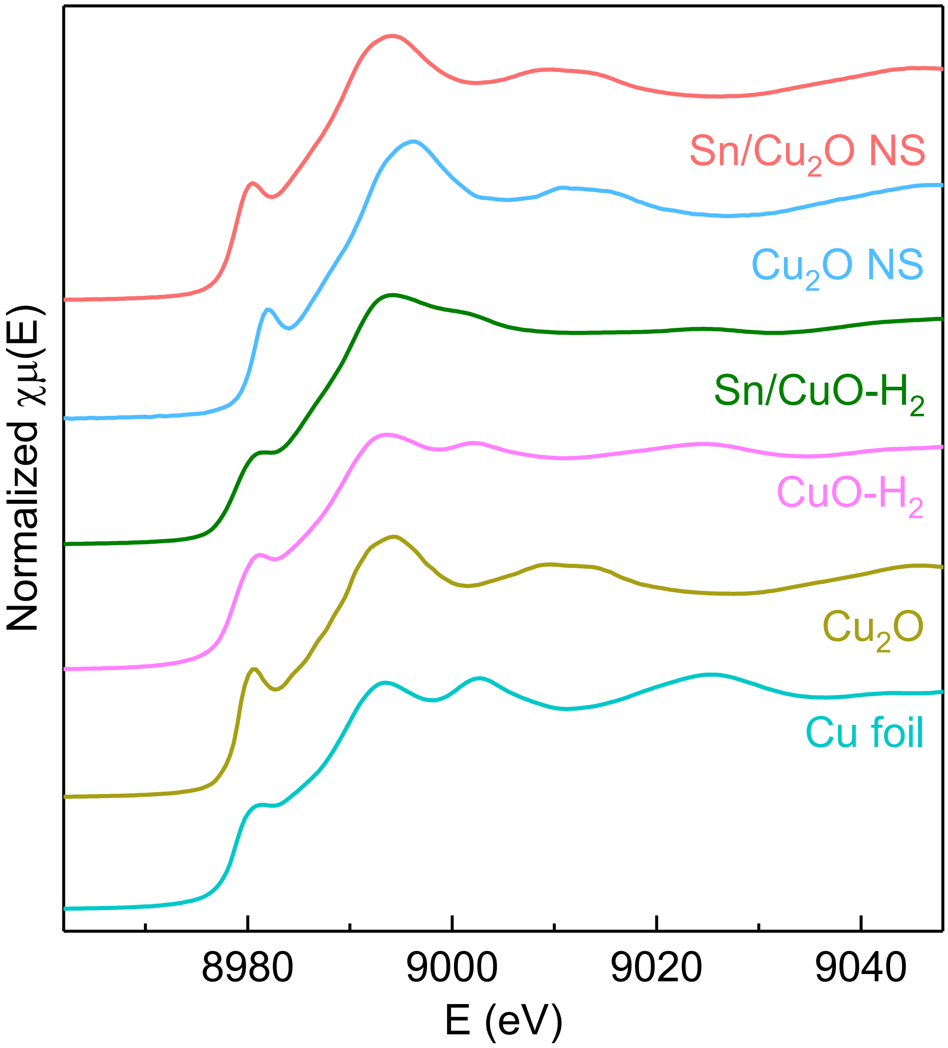

Figure S5. Co K-edge XANES experimental spectra of CuO-H_2, Sn/CuO-H_2 and the two before reaction with the data of Cu foil and Cu_2O as references.

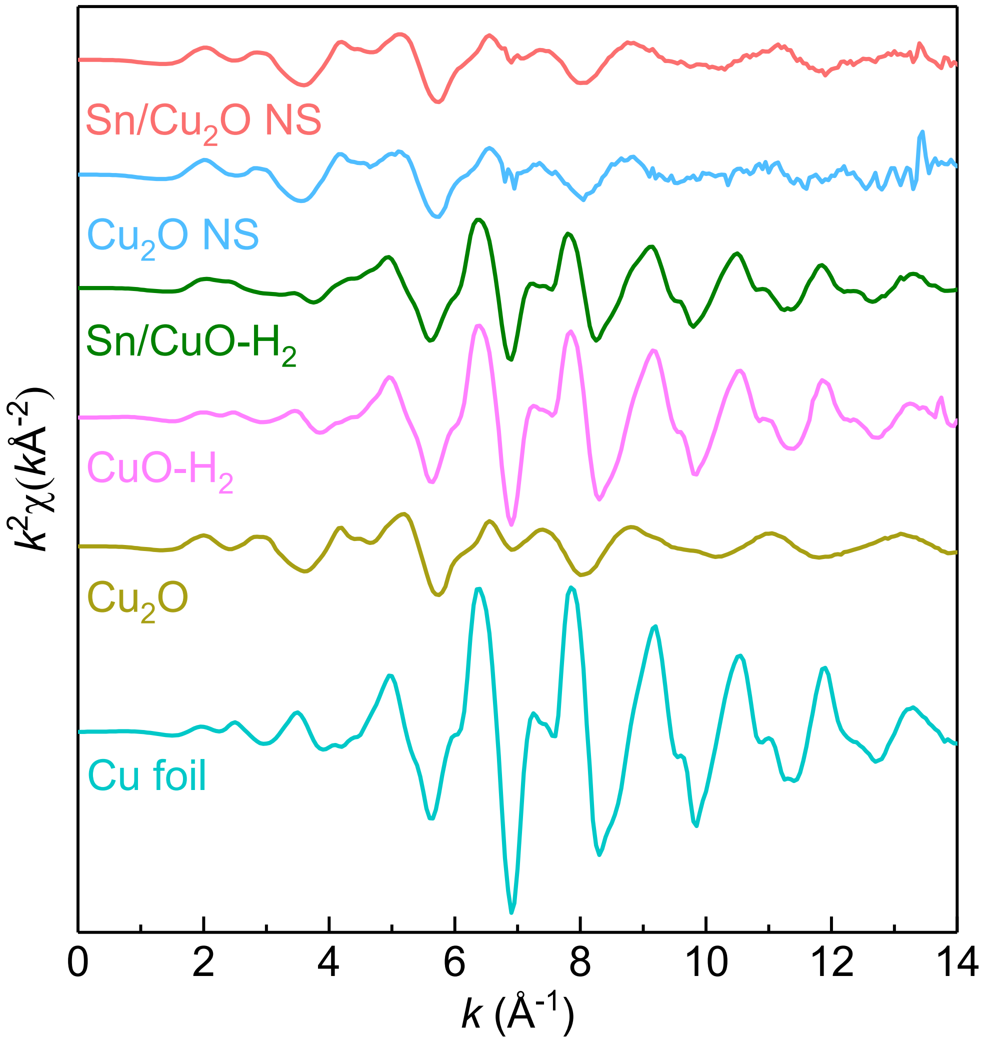

Figure S6. The corresponding Fourier transforms spectra of CuO-H_2, Sn/CuO-H_2 and the two before reaction with the data of Cu foil and Cu_2O as references.

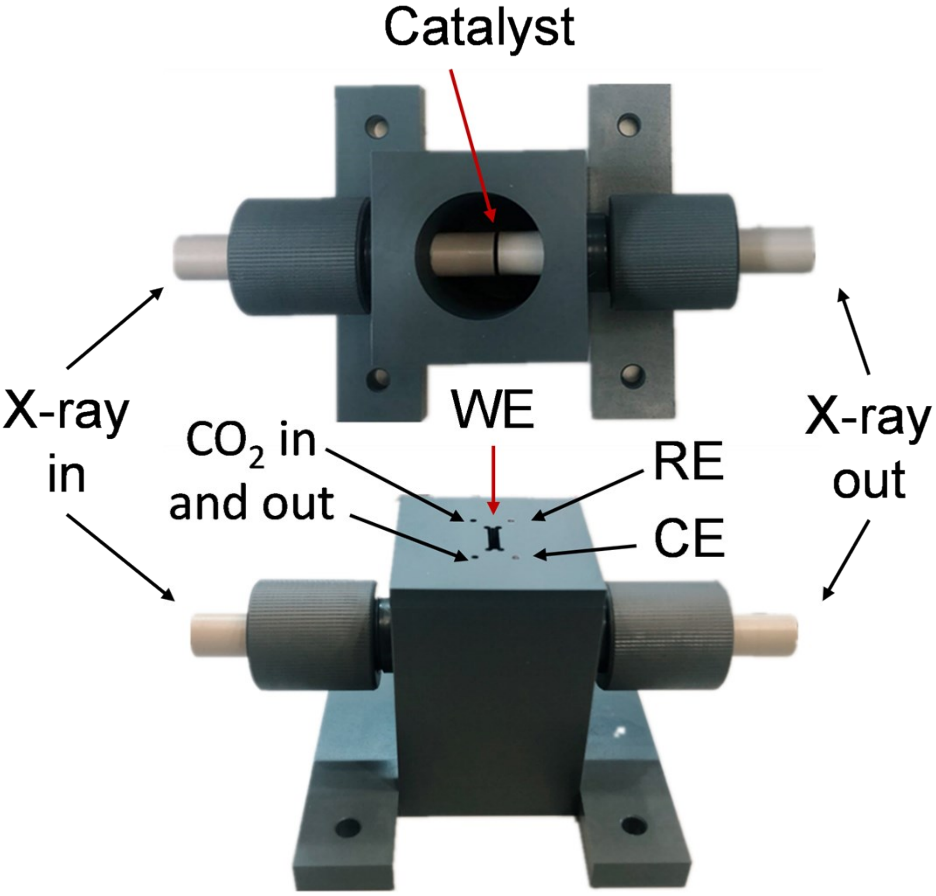

Figure S7. The electrochemical cell for operando transmission Quick-XAFS measurement. The catalysts were loaded on the carbon cloth as working electrode (WE), Ag/AgCl and platinum mesh were used for the reference electrode (RE) and counter electrode (CE), respectively.

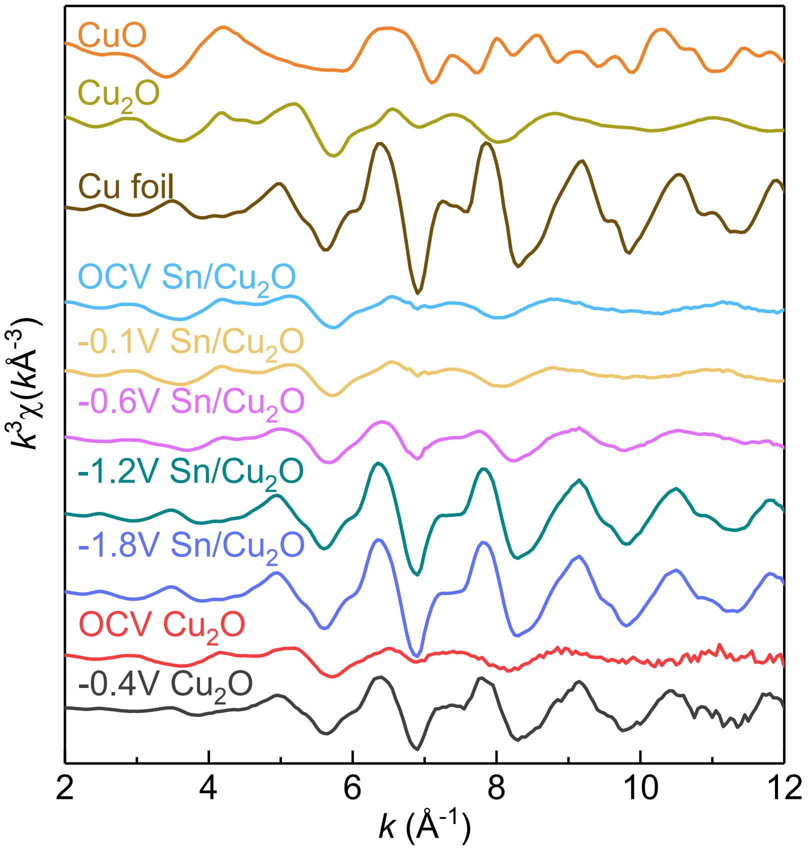

Figure S8. The $k^3\chi(k)$ oscillations of Cu K-edge operando EXAFS analysis for Cu_2O and Sn/Cu_2O in different potentials, with the data of CuO, Cu_2O and Cu foil as references.

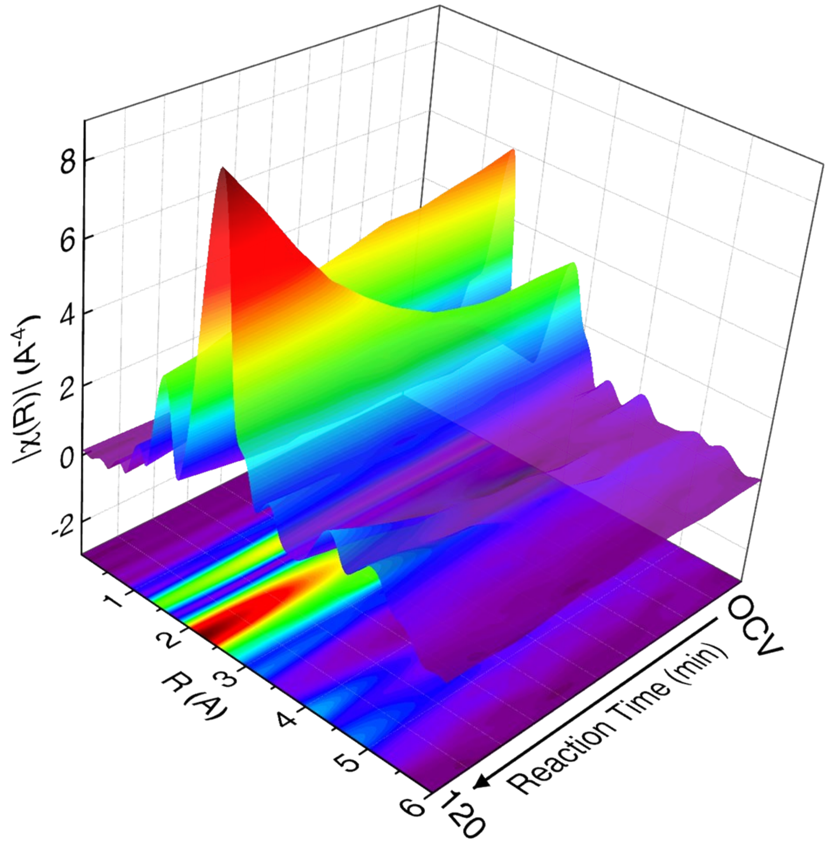

Figure S9. Three-dimensional profile plot of successive operando Cu *K*-edge EXAFS spectra acquired in different potentials, in corresponding to the XANES spectra in Fig. 2b.

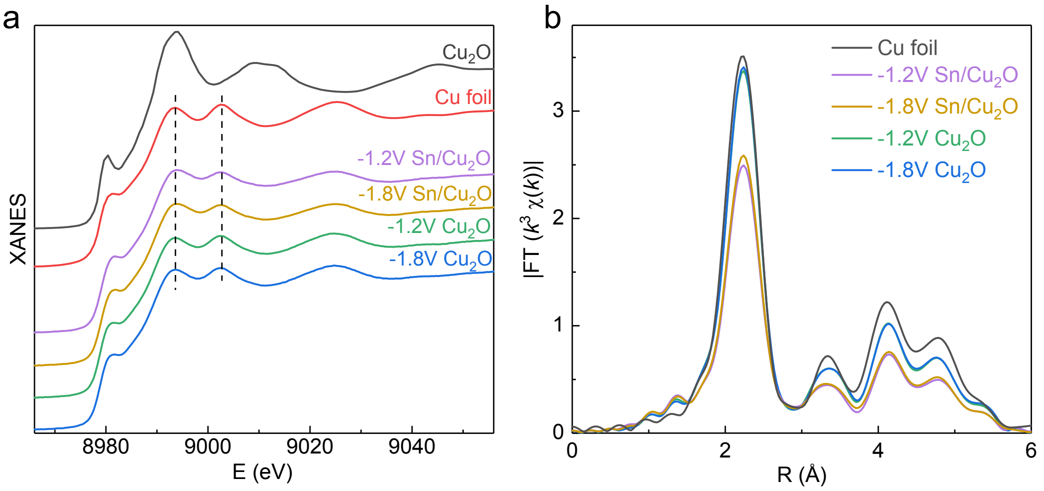

Figure S10. a, The *Operando* XANES spectra of Cu *K*-edge at -1.2V and -1.8V for Sn/Cu_2O and Cu_2O, and **b**, the Corresponding k^3-weighted FT spectra at Cu *K*-edge, respectively.

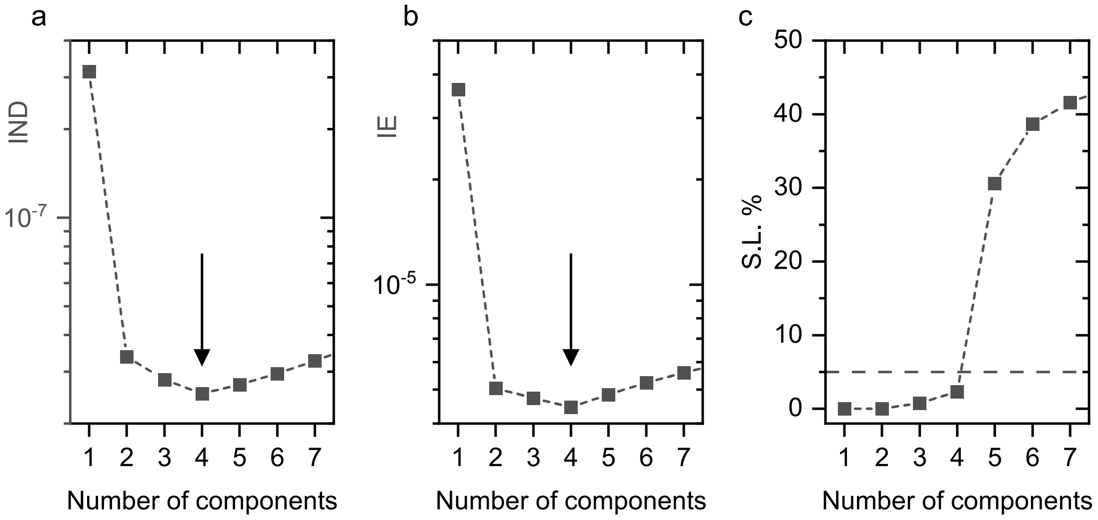

Figure S11. (a) IND function. (b) IE function. (c) *F*-test.

This Figures demonstrate the statistical estimators for the experimental dataset. IND (part a) and IE (part b) functions are expected to reach minimum when the number of components correspond to the real number of different species. In *F*-test (part c), the corresponding number of species is determined as the maximal number providing the value of function below 5%. Therefore, all three estimators indicate that the experimental dataset contains four independent components.

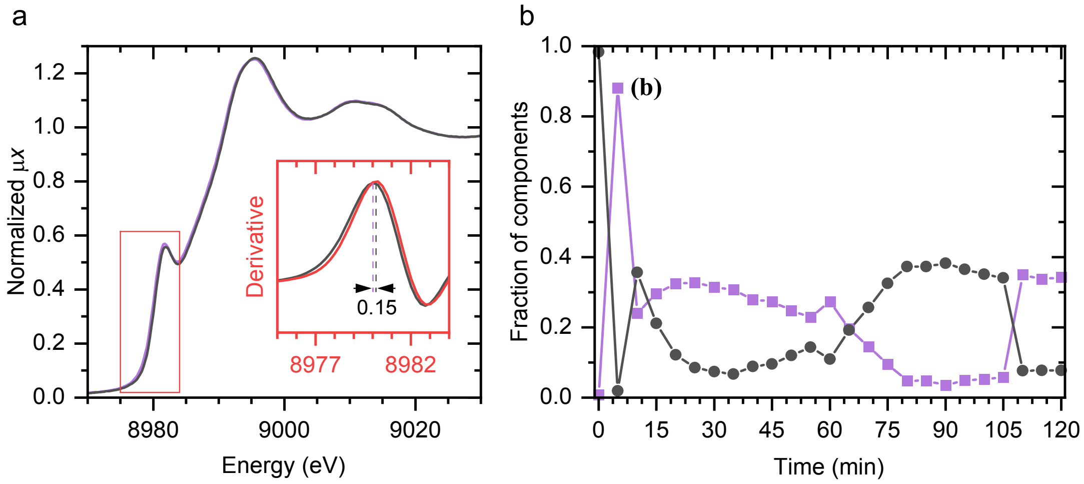

Figure S12. (a) XANES 1st and 4th components after the target transformation (The inset shows the derivative of the two spectra). (b) The corresponding concentration profile.

After the target transformation procedure was applied, two of these components appeared to be identical in shape and shifted by 0.15 eV with respect to each other (Fig. S11a). Their concentration profiles also interchange at several points (Fig. S11b). The above indicates that the two components should originate from the same copper species, but the small energy misalignment that can easily occur in experiment and may not be properly corrected by Athena software used to process the data result in an additional component in the statistical analysis.

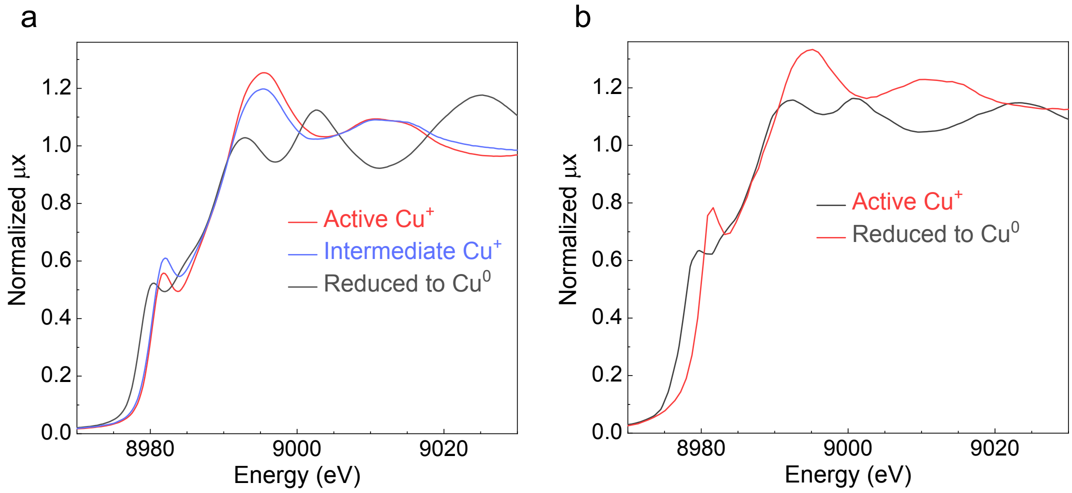

Figure S13. (a) and (b) XANES spectra after the target transformation for Sn/Cu_2O and Cu_2O electrocatalyst, respectively.

Therefore, three independent components were used for the further analysis. The results of the target transformation procedure with three components is shown in Supplementary Fig. 12a and b. The initial component (red lines) corresponds to Cu^+ similar to the Cu_2O reference.

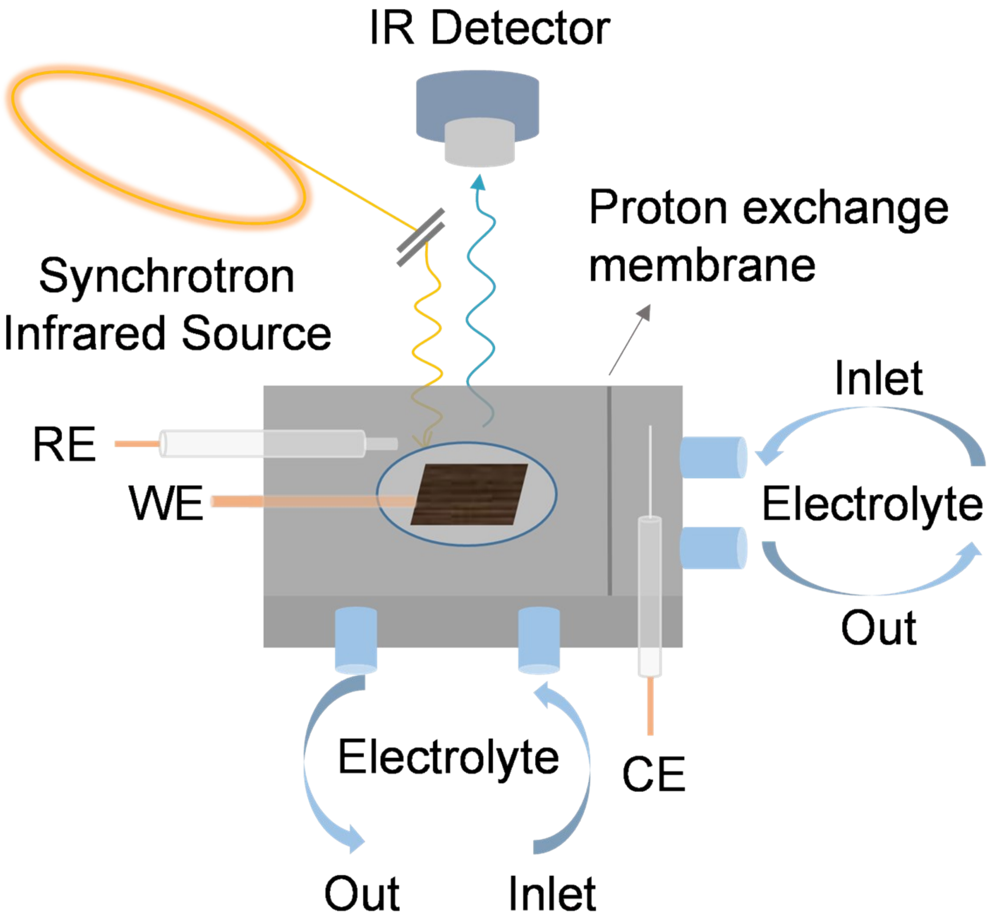

Figure S14. The electrochemical cell for operando FT-IR measurement. The catalysts were loaded on the carbon cloth as working electrode (WE), Ag/AgCl and platinum wire were used for the reference electrode (RE) and counter electrode (CE), respectively.

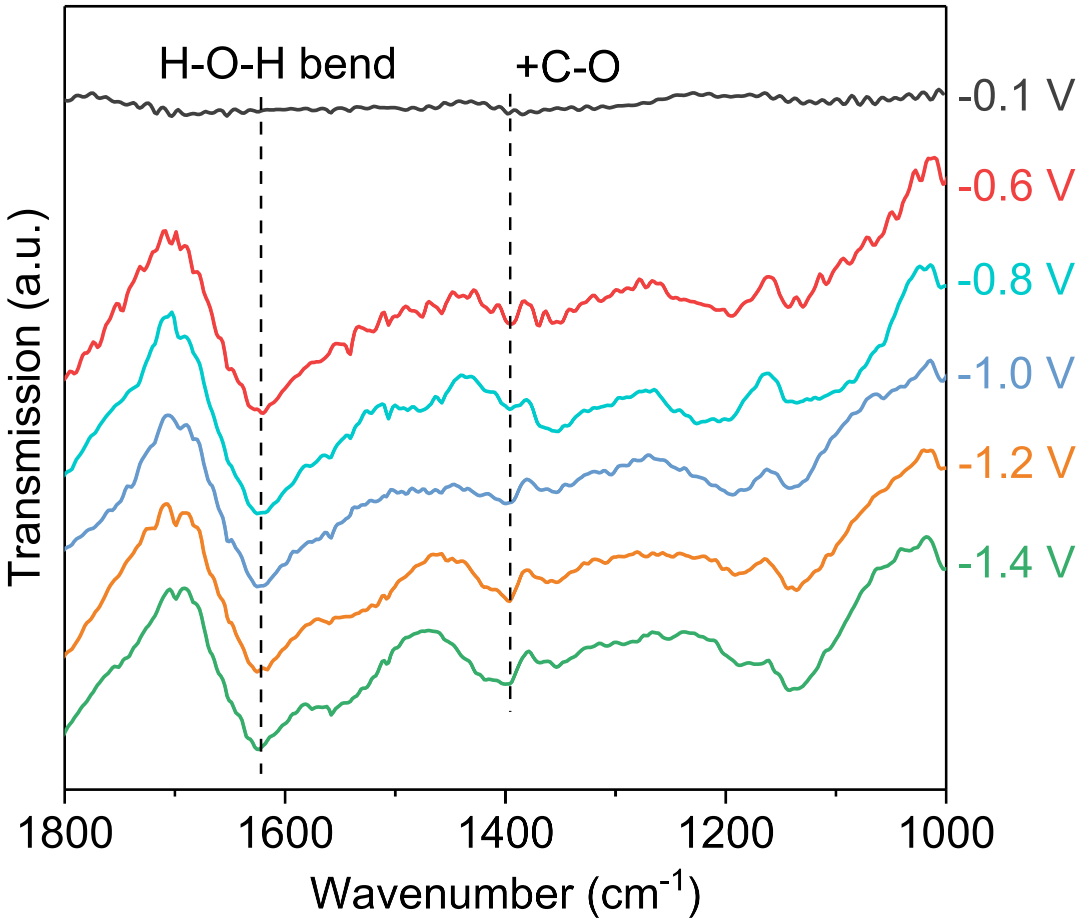

Figure S15. *Operando* FT-IR spectra of the pure Cu_2O NS at different applied voltages.

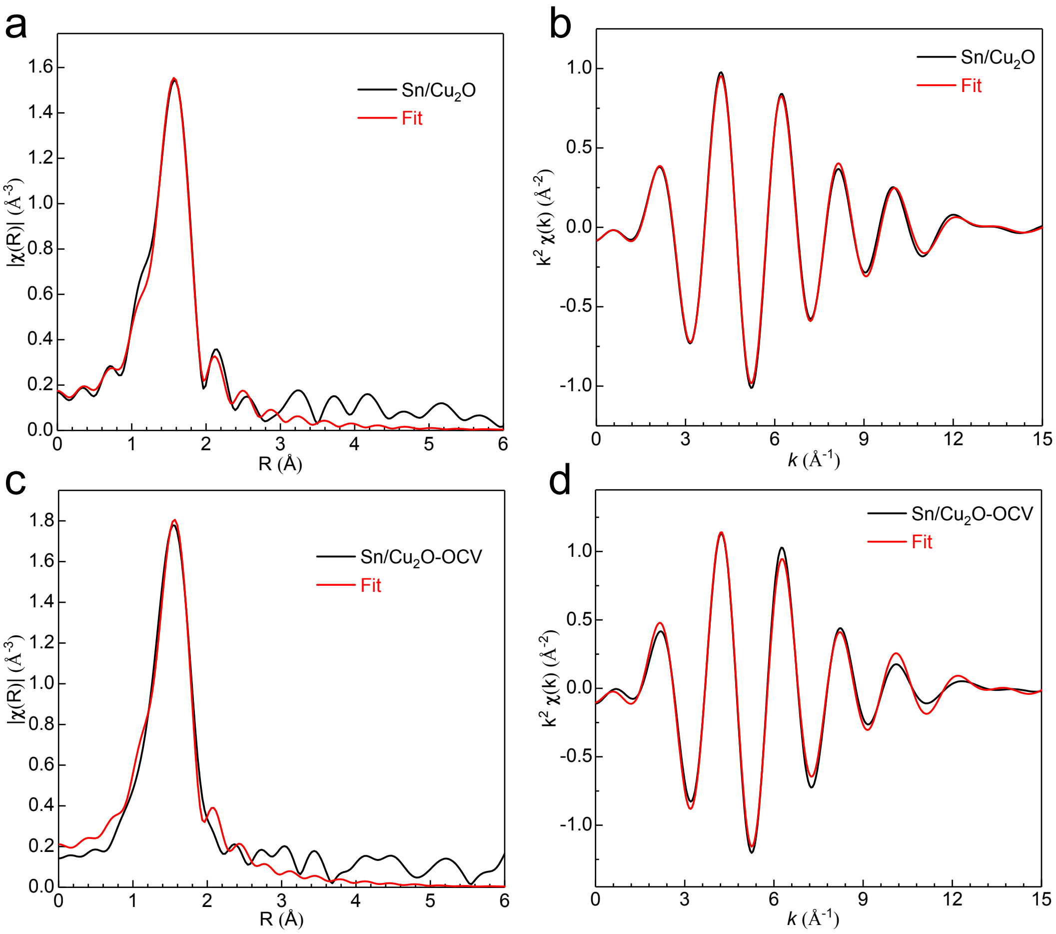

Figure S16. The fitting curve of k^2-weighted EXAFS spectra and $k^2\chi(k)$ oscillations of Sn/Cu_2O (a-b) and Sn/Cu_2O-OCV (c-d), using the ARTEMIS module of IFEFFIT.

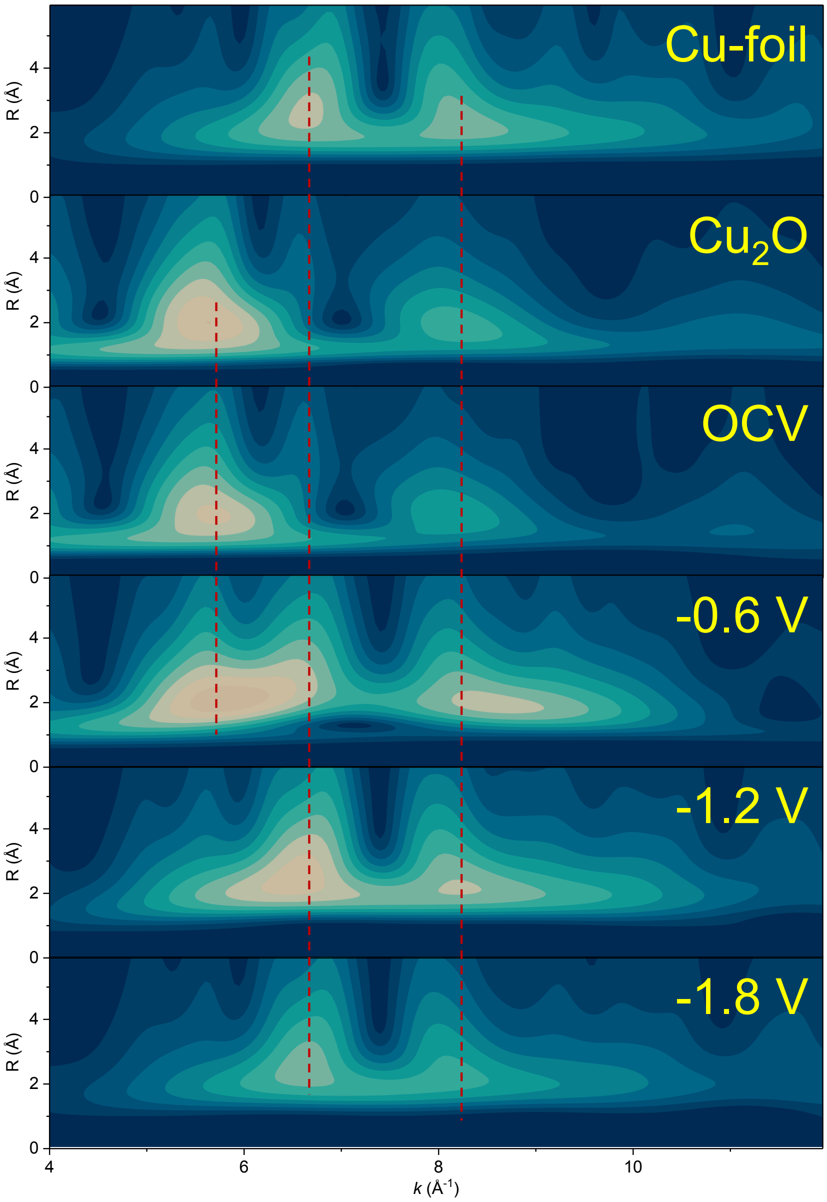

Figure S17. Wavelet transform contour spectra for the k^3-weighted EXAFS data of different conditions.

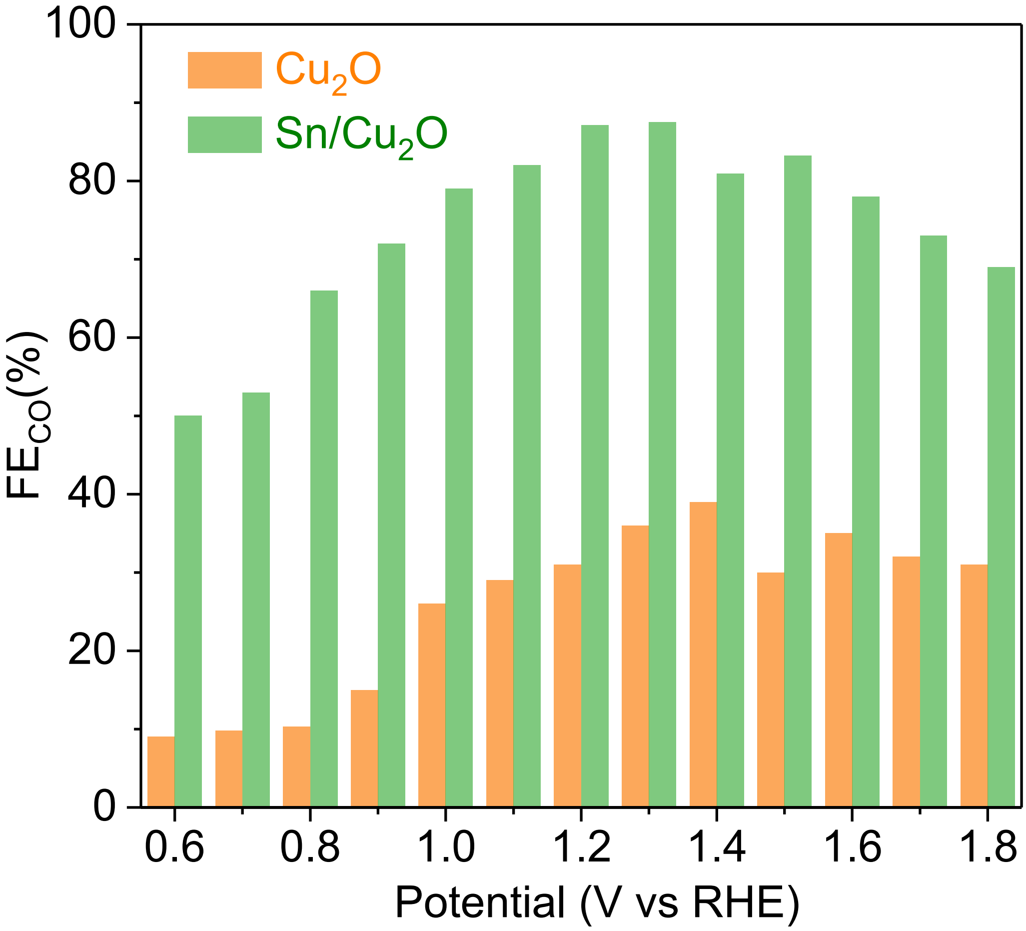

Figure S18. FE toward CO (FE_{CO}) for Cu_2O and Sn/Cu_2O NS at different applied potential from -0.6V to -1.8V vs RHE, respectively.

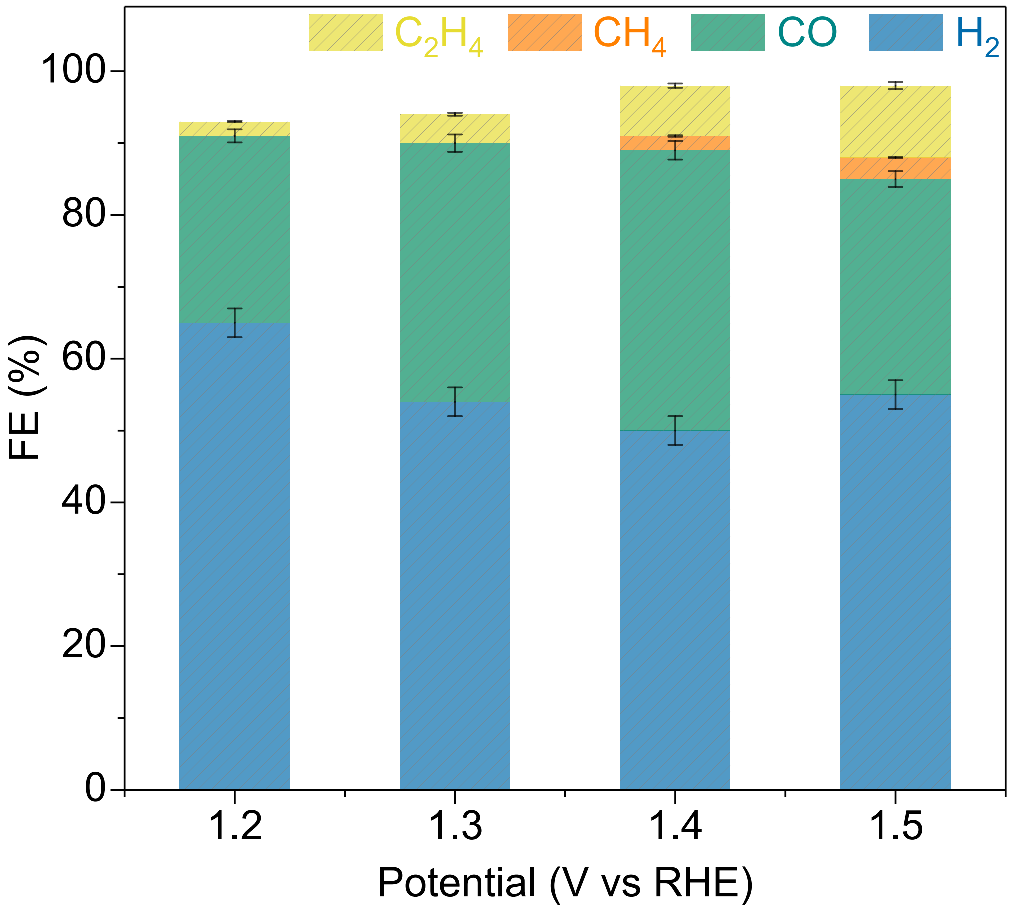

Figure S19. Faradaic efficiency for pure Cu_2O nanosheets.

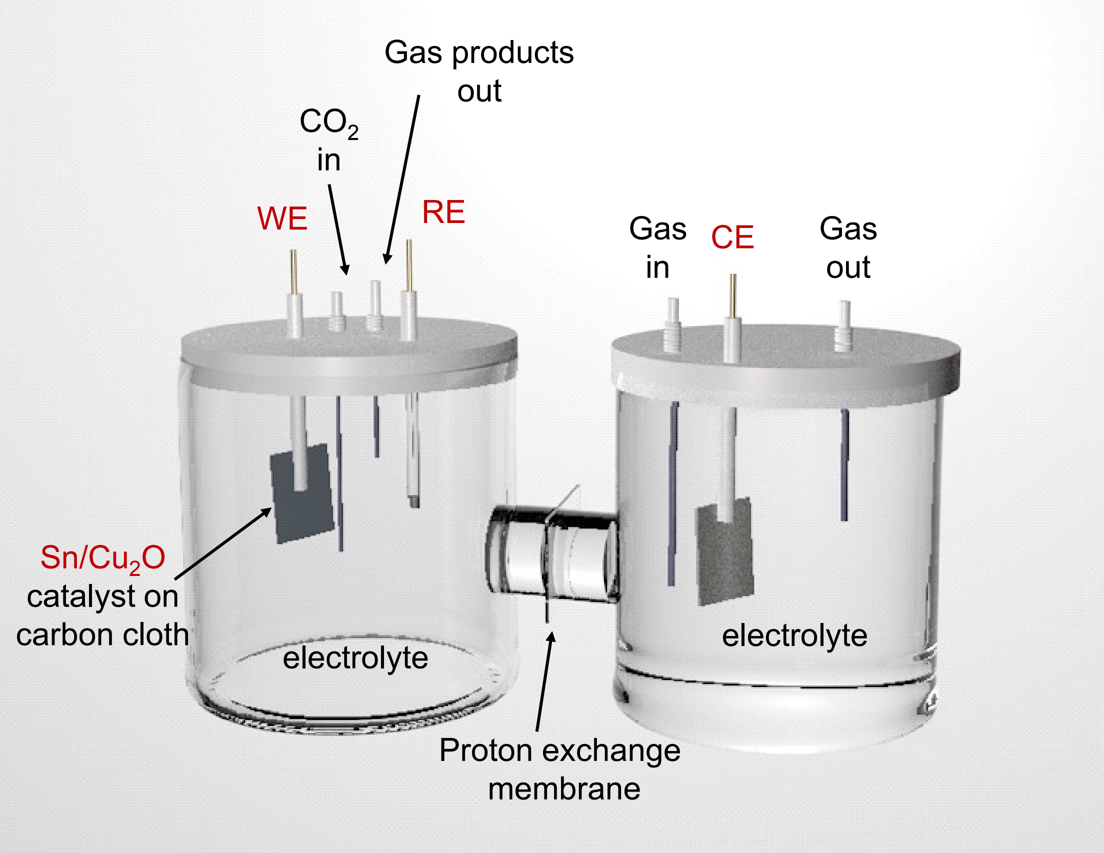

Figure S20. Exploded view of the H-cell electrolyzer for CO_2 electroreduction.

Table S1. Structural parameters at Sn *K*-edge extracted from quantitative EXAFS curve-fitting using the ARTEMIS module of IFEFFIT.

Sample	Path	CN	R(Å)	σ^2(10^{-3} Å)	ΔE_0(eV)	R-factor (10^{-3})
Sn/Cu_2O	Sn-O	5.00	2.05	3.3	9.02	3.24
Sn/Cu_2O-OCV	Sn-O	6.20	2.04	4.5	8.79	9.66

CN, coordination number; R, bonding distance; σ^2, Debye-Waller factor; ΔE_0, inner potential shift.

Reference

1 A. Martini, S. A. Guda, A. A. Guda, G. Smolentsev, A. Algasov, O. Usoltsev, M. A. Soldatov, A. Bugaev, Y. Rusalev, C. Lamberti, A. V. Soldatov, *Comput. Phys. Commun.*, 2020, **250**, 107064.

2 E. R. Malinowski, *Anal. Chem.*, 2002, **49**, 612-617.

3 E. R. Malinowski, *J. Chemom.*, 1989, **3**, 49-60.

4 P. Giannozzi, S. Baroni, N. Bonini, M. Calandra, R. Car, C. Cavazzoni, D. Ceresoli, G. L. Chiarotti, M. Cococcioni, I. Dabo, A. D. Corso, S. D. Gironcoli, S. Fabris, G. Fratesi, R. Gebauer, U. Gerstmann, C. Gougoussis, A. Kokalj, M. Lazzeri, L. M. Samos, N. Marzari, F. Mauri, R. Mazzarello, S. Paolini, A. Pasquarello, L. Paulatto, C. Sbraccia, S. Scandolo, G. Sclauzero, A. P. Seitsonen, A. Smogunov, P. Umari, R. M. Wentzcovitch, *J. Phys. Condens. Matter.*, 2009, **21**, 395502.